Dynamic Modeling and Simulation of Industrial Naphta Reforming Reactor

Gholamreza Zahedi, M. Tarin, M. Biglari

Abstract—This work investigated the steady state and dynamic simulation of a fixed bed industrial naphtha reforming reactors. The performance of the reactor was investigated using a heterogeneous model. For process simulation, the differential equations are solved using the 4th order Runge-Kutta method .The models were validated against measured process data of an existing naphtha reforming plant. The results of simulation in terms of components yields and temperature of the outlet were in good agreement with empirical data. The simple model displays a useful tool for dynamic simulation, optimization and control of naphtha reforming.

Keywords—Dynamic simulation, fixed bed reactor, modeling, reforming

I. INTRODUCTION

CATALYTIC reforming of naphtha is a major process to produce gasoline with high octane number in refinery and petrochemical industry. In this process paraffins and naphthenes are converted to aromatics by platinum catalyst. The catalytic reforming uses a bifunctional catalyst by which an acidic function (provided by a chlorinated alumina carrier) is combined with a hydrogenation/dehydrogenation function (provided by platinum with a second metal) [1]. The improvement in octane quality is mainly achieved by the formation and concentration of aromatic hydrocarbons as a result of a variety of reactions [2]. A simple model was suggested by Smith [3], in which naphtha reforming is considered as a combination of only four reactions. Ancheyta et al. [4] presented a kinetic equation which was incorporated in a fixed-bed uni-dimensional pseudo homogeneous adiabatic reactor model. Rahimpour et al. [5] presented kinetics and deactivation models for industrial catalytic naphtha reformers, as well.

A dynamic simulation of reforming process with catalyst regeneration and circulation was carried out by Lee et al. [6]. In their modeling, seven CSTRs (Continuous Stirred Tank Reactor) were used for each reactor and to account for catalyst deactivation each CSTR was divided into N fragments. The corresponding models were solved as a series of equations within each CSTR. The lifting gas flow rate was used in the dynamic simulation for controlling catalyst circulation and regeneration rate, and good agreement with plant data was achieved for both steady state and dynamic simulations.

A simulation model for catalytic reforming has been also developed by Padmavathi and Chaudhuri [7] to monitor commercial plant performance. The model involved 35 pseudo components.

G. Zahedi is with Process Systems Engineering Centre (PROSPECT), Faculty of Chemical Engineering, Universiti Teknologi Malaysia, UTM Skudai, 81310 Johor Bahru, Johor, Malaysia (Fax:+(6)-07-5581463; Email: grzahedi@cheme.utm.my, grzahedi@yahoo.com)

M. Tarin graduated from Chemical Engineering Department, Razi University, Iran.

M. Biglari is with Department of Chemical Engineering, Ryerson University, Toronto, Ontario, Canada M5B 2K3

Khosrvanipour, Mostafazadeh and Rahimpour [8] presented modeling and simulation of a catalytic membrane naphtha reformer. They showed that there are many advantages in using membrane reactors; including a lower temperature than customary fixed-bed reactors which results in longer life of catalysts and higher aromatic generation rate, among other positive effects.

Simulation of the naphtha reforming process needs information pertaining to reaction kinetics, as well as mass and heat transfer between gas phase and catalyst surface. Stijepovic et al. [9] presented a series of reliable kinetic data. Several other models have been also reported in the literature for naphtha reforming. Yet a critical inspection of the literature discloses that there is sparse amount of information available concerning the use of dynamic models for industrial naphtha reforming reactors in the face of catalyst deactivation. Consequently, this paper presents the results of a dynamic simulation of naphtha reforming in the presence of catalyst deactivation by a dynamic simulator.

II. PROCESS DESCRIPTION

Use Naphtha reforming process converts low octane gasoline to high octane number. Fig. 1 shows process flow diagram of the naphtha reforming process in Kermanshah refinery, Iran. The naphtha feed is mixed with rich hydrogen recycle gas and then is heated to desired temperature and enters the first reactor. The molar ratio of H2/HC must be kept at a specific level [10, 7]. Most of the reactions are endothermic and result in temperature drop across the reactor and reduction in the reactions rate. To avoid temperature decline, reactions take place in three reactors instead of one reactor [9]. The effluent of first reactor is reheated and is directed to second reactor in which mostly isomerization reactions take place. Outlet of second reactor after heating is entered to third rector. In this reactor dehydrocyclization and cracking occur; however, the temperature drop across the third reactor is marginal because of exothermic behavior of the reactions. The outlet of third reactor is then cooled and separated to liquid and gas phases in a high pressure separator drum. The gas phase which is rich in hydrogen is recycled and the liquid phase after stripping from some light gases is sent to gasoline tanks.
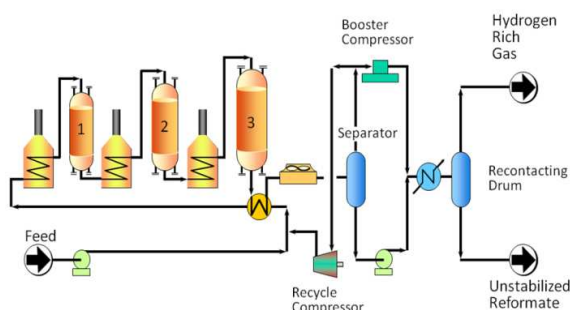

Fig. 1 Process flow diagram for Naphtha reforming [10]

Tables I and II exhibit the characteristics of the studied industrial naphtha reforming reactor.
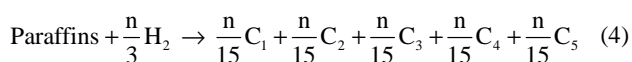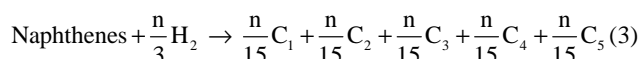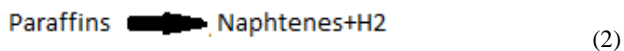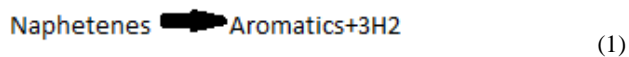
TABLE I
CATALYST SPECIFICATION [10]

Parameter	Value
Pt (wt%)	0.3
Re (wt%)	0.3
a_v (m.h^{-1})	220
Void fraction of bed	0.36
Density of bed catalyst (kg.l^{-1})	0.3
Catalyst diameter (mm)	1.2

TABLE II
SPECIFICATIONS OF THE REACTORS [10]

PARAMETER	VALUE
Naphtha (kg/h)	30.41×10^3
H$_2$/HC molar ratio	4.74
Mole percent of H$_2$ in recycle	69.5
Diameter and Length of first reactor (M)	1.52 , 6.29
Diameter and Length of second reactor (M)	1.67 , 7.13
Diameter and Length of third reactor (M)	1.98 , 7.89

III. REACTION KINETICS

There were few kinetic models with industrial application. Among the models the kinetics proposed by smith [3] was employed in our study. In this kinetic model, naphtha reforming is summarized as the main fractions of aromatics, paraffins and naphthenes. Four main reactions are dehydrogenation on naphthenes, dehydrocyclization of paraffins, hydrocracking of naphthenes and hydrocracking of paraffins. The four reactions are given as the following [3]:

$$\text{Naphetenes} \rightleftharpoons \text{Aromatics} + 3H2 \qquad (1)$$

$$\text{Paraffins} \rightleftharpoons \text{Naphtenes} + H2 \qquad (2)$$

$$\text{Naphthenes} + \frac{n}{3}H_2 \rightarrow \frac{n}{15}C_1 + \frac{n}{15}C_2 + \frac{n}{15}C_3 + \frac{n}{15}C_4 + \frac{n}{15}C_5 \quad (3)$$

$$\text{Paraffins} + \frac{n}{3}H_2 \rightarrow \frac{n}{15}C_1 + \frac{n}{15}C_2 + \frac{n}{15}C_3 + \frac{n}{15}C_4 + \frac{n}{15}C_5 \quad (4)$$

Accordingly, the rates of reactions are determined as follows [3, 8]:

$$R_1 = \frac{k_1}{K_1}(K_1 P_n - P_a P_h^3) \qquad (5)$$

$$R_2 = \frac{k_2}{K_2}(K_2 P_n P_h - P_p) \qquad (6)$$

$$R_3 = \frac{k_3}{P_t}(P_n) \qquad (7)$$

$$R_4 = \frac{k_4}{P_t}(P_p) \qquad (8)$$

Where R_1, R_2, R_3 and R_4 are reaction rates of naphtha reforming respectively. P_i (i = paraffins, aromatics, naphthenes and H$_2$) is a partial pressure of component i. k_1, k_2, k_3 and k_4 are the rate coefficient of reaction, respectively, while K_1, K_2, K_3 and K_4 are equilibrium constants of the reactions, respectively. The expressions of these parameters are given as below [3].

$$K_1 = 1.04 \times 10^{-3} \exp(46.15 - 50784/1.8T) \qquad (9)$$

$$K_2 = 9.87 \exp(-7.12 + 8000/1.8T) \qquad (10)$$

$$k_1 = 9.87 \exp(23.21 - 34750/1.8T) \qquad (11)$$

$$k_2 = 9.87 \exp(35.98 - 59600/1.8T) \qquad (12)$$

$$k_3 = k_4 = \exp(49.97 - 62300/1.8T) \qquad (13)$$

IV. MATHEMATICAL MODEL

The catalyst deactivation gives unsteady state behavior to the process and the reactors; therefore, in order to build dynamic model of the reactor the following assumptions were made:

1) One dimensional plug flow is considered.
2) Axial dispersion of heat is neglected compared to convection term.
3) There are no radial concentration and temperature gradients.

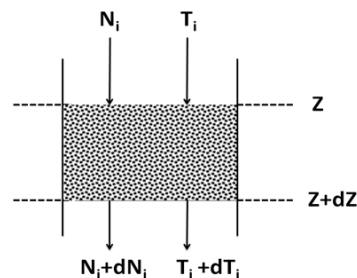Fig. 2 shows an element along the reactors bed for applying governing equations.

Fig. 2 An element of length Δz, in the tubular reactor

Mass and energy balance for the fluid phase are expressed by:

$$\varepsilon_b c_t \frac{\partial y_i}{\partial t} = -c_t \frac{\partial(u y_i)}{\partial z} - K_{gi} a_V c_t y_i - y_{is} \qquad (14)$$

$$\varepsilon_b c p_g c_t \frac{\partial T}{\partial t} = -c p_g c_t \frac{\partial T}{\partial Z} - h a_V (T - T_s) \qquad (15)$$

The following two conservations equations are written for the solid phase:

$$\varepsilon_s c_t (1 - \varepsilon_b) \frac{\partial y_{is}}{\partial t} = K_{g_i} a_V c_t (y_i - y_{is}) - a r_i \rho_b \qquad (16)$$

$$c p_s \rho_b \frac{\partial T_s}{\partial t} = h a_V (T - T_s) + \sum_{i=1}^{3} (-\Delta H_r) a r_i \rho_b \qquad (17)$$

The boundary conditions are as follows:

$$z = 0 \; ; \quad y_i = y_{i0} \, , \; T = T_0 \qquad (18)$$

$$t = 0; \; y_i = y_i^s \, , \; y_{is} = y_{is}^s \, , \; T = T^s \, , \; T_s = T_s^s \, , \; a = 1 \qquad (19)$$

A. Deactivation Model

The catalyst deactivation model for commercial naphtha reforming has been used from Ref. [11] as:

$$\frac{da}{dt} = -k_{Act} \exp\left(\frac{-E_{Act}}{RT}(\frac{1}{T} - \frac{1}{T_r})\right)a^n \qquad (20)$$

B. Heat and Mass Transfer Coefficients

Mass transfer coefficient between gas phase and solid phase is given by the following equation [12]:

$$k_{gi} = \frac{0.458}{\varepsilon_b}(Re_p)^{-0.407}(0.123\rho D_{im}/\mu)^{(-2/3)} \qquad (21)$$

And heat transfer coefficient between gas phase and solid phase was obtained from Ref. [13] as below:

$$h_i = 0.2G\,C_{pg}\,Re_{di}^{-0.2}\,Pr^{(-2/3)} \qquad (22)$$

C. Numerical Solution

In order to investigate effect of process parameters on production rate, the set of partial differential equations, ordinary differential equations of deactivation model, non linear algebraic equations of reaction rates and auxiliary correlations should be solved numerically. In this case, the equations initially were solved based on our previous experience on the process steady state model by setting time derivatives in Equations 14-17 to zero and considering the activity to be unity.

So by using backward finite difference method the steady state simulation are converted to nonlinear algebraic equations [14]. The reactor was separated into several segments and then Gauss–Newton method was utilized to solve the nonlinear algebraic equations in each segment [14]. The consequence of the steady state simulation was utilized as the initial conditions for dynamic state equations in each node of the reactor. In order to solve a dynamic simulation the set of equations have been separated in axial coordinate on the nodes so partial differential equations are altered to ordinary differential equations. The 4th order Runge–Kutta approximation was used to solve ordinary differential equations. All programs were carried out in MATLAB 7.5 software [15].

V. RESULTS AND DISCUSSIONS

A. Steady-state Module

In order to investigate the validation of steady state model, the consequence of steady state simulation and plant data at zero time are given in Table III. Fig. 3 to 7 display the mole fraction of reactants, products and temperature for gas phase along the reactor resulting from steady state simulation. From Fig. 3 and Fig. 4, paraffin and naphthen mole fractions decrease while in Fig. 5 and Fig. 6, aromatic and hydrogen mole fractions increase along the reactor. Fig. 7 shows temperature profile of gas phase along the reactor.

TABLE III
COMPARISON BETWEEN SIMULATED RESULTS AND PLANT DATA FOR FRESH CATALYST [10]

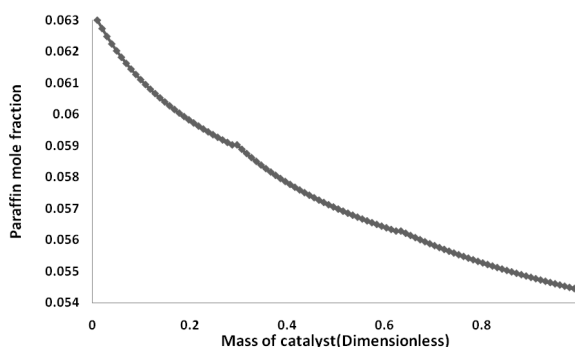| Reactor	Outlet Temperature (K)		Aromatic in Reformate (mole %)	
	Plant	Simulation	Plant	Simulation
1	759	760	-	0.29
2	765	766	-	0.41
3	772	769.5	0.48	0.5

Fig. 3 Paraffin mole fraction profile along the reactor axis for fluid phase under steady state condition
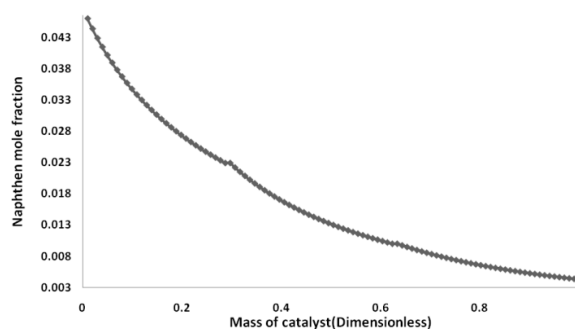

Fig. 4 Naphthen mole fraction profile along the reactor axis for fluid phase under steady state condition
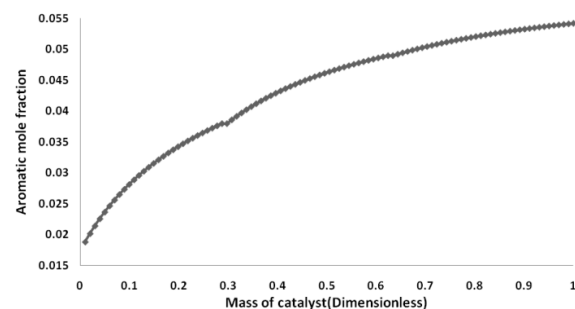

Fig. 5 Aromatic mole fraction profile along the reactor axis for fluid phase under steady state condition
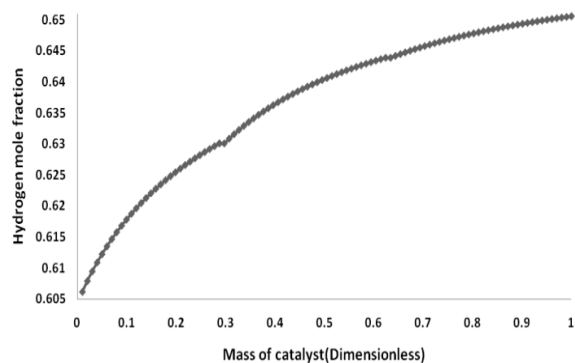
Fig. 6 H$_2$ mole fraction profile along the reactor axis for fluid phase under steady state condition

B. Dynamic Module

Table V indicates validation of dynamic model for reformate production rate. It was illustrated that, there is a good agreement between dynamic simulation results and historical process data from [10]. Fig. 8 to 12 shows the three dimensional gas phase components and activity of the catalyst along the rector during operation time of naphtha reforming reactors. Fig. 8 and 9 illustrate the aromatic and hydrogen mole fractions versus time and length for naphtha reforming reactors, respectively. The mole fractions of aromatics and hydrogen increase along the reactor, while they decrease as time passes due to catalyst deactivation.
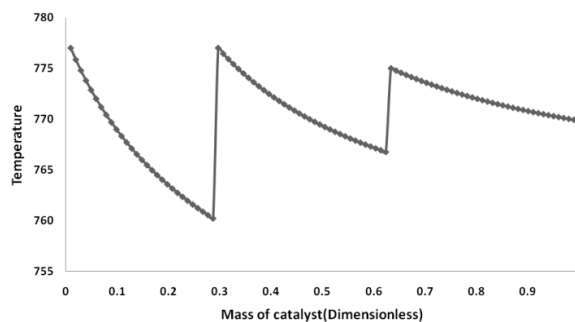

Fig. 7 Temperature mole fraction profile along the reactor axis for fluid phase under steady state condition
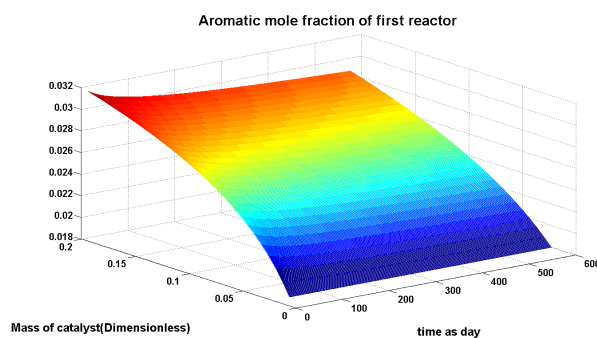

Fig. 8 Aromatic mole fraction of first reactor as a function of length and time
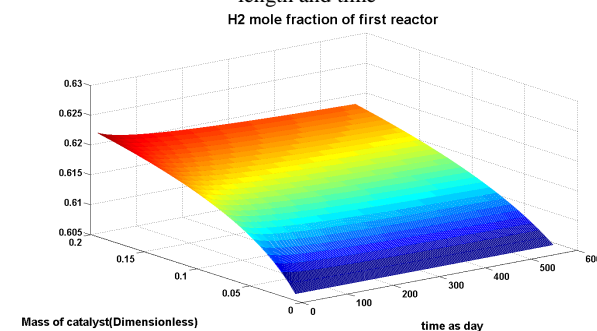

Fig. 9 H$_2$ mole fraction of first reactor as a function of length and time

TABLE IV
COMPARISON BETWEEN PREDICATED REFORMATE PRODUCTION RATE WITH PLANT DATA PRODUCTION RATE

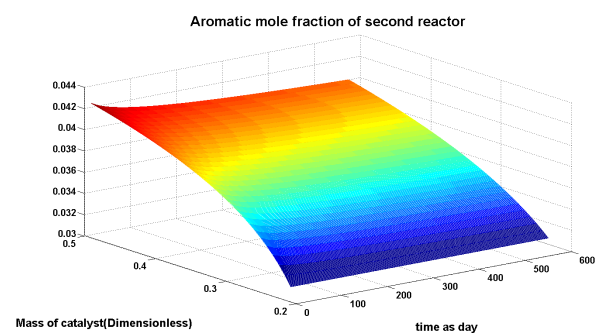| Day	Industrial data (ton/day)	Simulation result (ton/day)	Error (%)
0	225.90	212.70	5.8
34	224.25	216.32	3.5
62	229.65	220.15	3.8
97	229.65	223.60	4.1
125	229.65	226.04	2.6
160	211.60	205.71	1.6
188	222.75	218.07	2.1
223	233.05	226.10	2.9
243	228.65	221.70	7.8
321	227.64	222.33	2.3
398	317.30	3.6.64	3.3
425	317.94	308.95	2.8
461	317.94	309.26	2.7
490	317.94	301.23	5.3
524	317.04	302.70	3.1
567	317.94	304.39	4.3
610	313.90	304.65	2.9

Fig. 10 Aromatic mole fraction of second reactor as a function of length and time
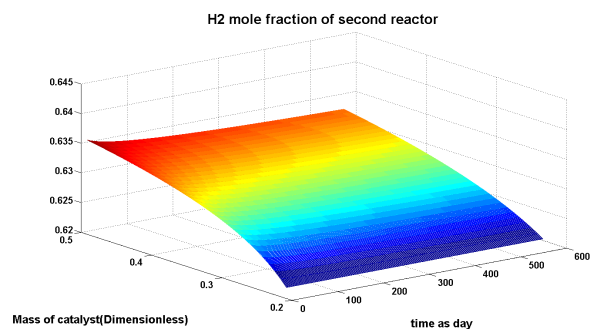
Fig. 11 H_2 mole fraction of second reactor as a function of length and time
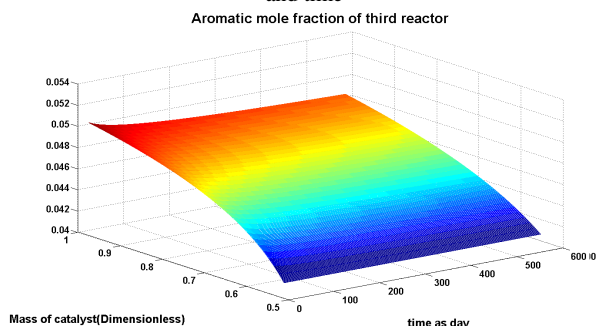

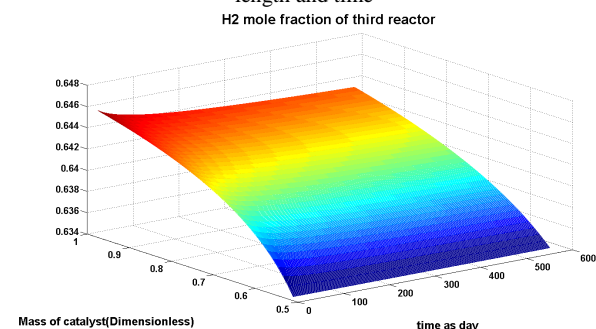Fig. 12 Aromatic mole fraction of second reactor as a function of length and time

Fig. 13 H_2 mole fraction of second reactor as a function of length and time

VI. CONCLUSIONS

An industrial naphtha reforming reactor was modeled and also simulated by the heterogeneous model. The proposed model has been solved numerically using the 4th order Runge–Kutta approach. Alteration of components and temperature, with time and reactor length was evaluated. Moreover, the model was validated with a typical plant industrial data. The model performed satisfactorily well at industrial conditions and a good agreement between the plant data and the simulation results was obtained.

ACKNOWLEDGMENT

NOMENCLATURE

ΔH_i	enthalpy change of reaction i(kJ/mol)
a_v	external particle surface area per unit of reactor volume ($m^2_s.m^{-3}_r$)
a	activity of catalyst (-)
cp_g	Specific heat of the gas at constant pressure ($kj.mol^{-1}.K^{-1}$)
cp_s	Specific heat of the solid at constant pressure ($kj.kg^{-1}.K^{-1}$)
c_t	total concentration ($mole.m^{-3}$)
E_{Act}	activation energy used in the deactivation model ($j.mole^{-1}$)
G	Superficial gas flow rate ($m.h^{-1}$)
h_i	gas inside heat transfer coefficient ($kj.m^{-2}.K^{-1}.h^{-1}$)
k_{Act}	deactivation model parameter constant (h^{-1})
K_{gi}	mass transfer coefficient for component i ($m.h^{-1}$) adsorption constants for CH_4 ,CO and H_2 (bar^{-1})
K_{H2O}	dissociative adsorption constant of H_2O(-)
K_1,	equilibrium constant (MPa^{-3})for reaction (1) and (MPa^{-1})
K_3	for reaction (2)
K_2	equilibrium constant of reaction 2(-)
k_i	forward rate constant ($kmol.h^{-1}.kg^{-1}.MPa^{-1}$) for reaction (1) and ($kmol.h^{-1}.kg^{-1}.MPa^{-2}$) for reaction (2) and ($kmol.h^{-1}.kg^{-1}$)for reactions (3) and (4)
n	sintering order(-)
p_i	Partial pressure of component i(bar)
R	universal gas constant ($j.mol^{-1}.K^{-1}$)
R_i	rates of reactions 1, 2 and 3 ($kmole.kg^{-1}.hr^{-1}$)
Re_d	Reynolds number of tube(-)
Re_p	Reynolds number of particle(-)
T	bulk gas phase temperature (K)
T_s	temperature of gas on the solid surface (K)
t	time (h)
u	superficial velocity ($m.h^{-1}$)
y_i	bulk gas phase mole fraction for component i (-)
y_{is}	Surface mole fraction of ith component in the solid phase (-)
Z	axial reactor coordinate (m)

Greek letters

ε_b	void fraction of catalytic bed ($m^3_g.m^{-3}_r$)
ε_s	solid particles' void fraction ($m^3_g.m^{-3}_s$)
ρ	density of gas mixture(Kg. m^{-3})
ρ	bed density of catalyst(Kg. m^{-3})
μ	Viscosity of gas mixture($kg.m^{-1}.h^{-1}$)

Superscripts and subscripts

0	inlet conditions
s	initial conditions

REFERENCES

[1] V.A. Mazzieri, C.L. Pieck, C.R. Vera, J.C. Yori, J.M. Grau, Effect of Ge content on the metal and acid properties of Pt-Re-Ge-Al$_2$O$_3$-Cl catalysts for naphtha reforming. Applied Catalysis A: General, 353: 93-100, 2009.
[2] A.V. Sapre. Catalyst deactivation kinetics from variable space velocity experiments. Chemical Engineering Science, 52(24): 4615-4623, 1997.
[3] R.B. Smith, Kinetic analysis of naphtha reforming with platinum catalyst. Chem. Eng. Prog. 55(6): 76–80 (1959).
[4] J. Ancheyta, E. Villafuerte, P. Schachat, R. Aguilar, E. Gonzalez. Simulation of a commercial semiregenerative reforming plant using feedstocks with and without benzene precursors, Chem. Eng. Technol. 25(5): 541-546, 2002.
[5] M.R. Rahimpour, S. Esmaili, G.N.A. Bagheri, Kinetic and deactivation model for industrial catalytic naphtha reforming. Iran. J. Sci. Technol., Trans. B: Tech. 27: 279–290, 2003.

[6] J.W. Lee, Y.C. Ko, Y.K. Jung, K.S. Lee, E.S. Yoon, A modeling and simulation study on a naphtha reforming unit with catalyst circulation and regeneration system. Comput. Chem. Eng. 21: S1105–S1110, 1997.

[7] G. Padmavathi, K.K. Chaudhuri, Modeling and simulation of commercial catalytic naphtha reformers. Can. J. Chem. Eng., 75(10): 930-937, 1997.

[8] A. Khosravanipour Mostafazadeh, M.R. Rahimpour. A membrane catalytic bed concept for naphtha reforming in the presence of catalyst deactivation. Chemical Engineering and Processing: Process Intensification, 48: 683-694, 2009.

[9] M.Z. Stijepovic, A. Vojvodic-Ostojic, I. Milenkovic, P. Linke. Development of a kinetic model for catalytic reforming of naphtha and parameter estimation using industrial plant data. Energy & Fuels, 23: 979-983, 2009.

[10] Kermanshah refinery Complex, "Operating data sheets of naphtha reforming plant", 2003–2008.

[11] C.H. Bartholomew. Mechanisms of catalyst deactivation. Applied Catalysis A: General 212: 17-60, 2001.

[12] R. Perry, D. Green, J. Maloney. Perry's chemical engineers' handbook. 6th ed., New York: McGraw Hill, 1984.

[13] S. Yagi, N. Wakao. Heat and mass transfer from wall to fluid in packed beds. AIChE .J 5(1): 79-85, 1959.

[14] S. Chapra, R. Canale. Numerical Methods for Engineers. 6th ed., New York: McGraw Hill, 2010.

[15] MATLAB, the Language of Technical Computing, Version 7.5. August 15, 2007, License Number: 34912, Copyright 1984–2007, the Math Works, Inc.